Thymosin β4 induces folding of the developing optic tectum in the chicken (Gallus domesticus)

ARTICLE *in* THE JOURNAL OF COMPARATIVE NEUROLOGY · JUNE 2012

Impact Factor: 3.23 · DOI: 10.1002/cne.23004 · Source: PubMed

Thymosin β4 Induces Folding of the Developing Optic Tectum in the Chicken (*Gallus Domesticus*)

Hans-Georg Wirsching,[1]* Oliver Kretz,[2] Gabriela Morosan-Puopolo,[1,3] Petya Chernogorova,[1] Carsten Theiss,[3] and Beate Brand-Saberi[1,3]*

[1]Department of Molecular Embryology, University of Freiburg, D-79104 Freiburg, Germany
[2]Department of Neuroanatomy, University of Freiburg, D-79104 Freiburg, Germany
[3]Department of Anatomy and Molecular Embryology, Ruhr University Bochum, D-44801 Bochum, Germany

ABSTRACT

Thymosin β4 (Tβ4) is a highly conserved G-actin binding polypeptide with multiple intra- and extracellular functions. While stem-cell activation as well as promotion of cell survival and migration by Tβ4 have been investigated in various in vitro and in vivo studies, there are few data on the implications of Tβ4 in brain development. In the present study we analyzed Tβ4 expression in the developing optic tectum of the chicken (*Gallus domesticus*) and performed in ovo retroviral transduction and plasmid electroporation for overexpression and knockdown of Tβ4. We found marked Tβ4 expression in the tectal plate and in all neuronal layers of later developmental stages, but not in the ventricular zone where neural stem cells reside and divide. Knockdown of Tβ4 inhibited growth of Tβ4-depleted hemispheres, whereas overexpression of Tβ4 led to the production of neuroepithelial folds resembling gyri and sulci, which are not normally present in avian brains. The mechanism yielding enhanced growth of Tβ4 overexpressing hemispheres involved enhanced proliferation, thus indicating an impact of Tβ4 on the neural stem cell and/or progenitor cell population. In summary, we found that due to its effects on proliferation, Tβ4 expression has a large impact on neuroepithelial and macroscopic brain development. J. Comp. Neurol. 520:1650–1662, 2012.

INDEXING TERMS: brain development; actin binding polypeptide; neural stem cell proliferation; neuroepithelium

Like the mammalian neocortex (NC), the chicken optic tectum (OT) is anatomically and functionally organized in horizontal layers and vertical columns (Gray et al., 1990). Consequently, NC and OT share basic developmental mechanisms, including proliferation predominantly within the ventricular zone, long-distance tangential migration, or migration within a functional column along radial glial processes (Gray et al., 1988; Gray and Sanes, 1991, 1992). However, convolutions of the brain surface—with crests known as gyri and grooves called sulci—normally occur exclusively in higher mammals as a result of the phylogenetic expansion of the cortical surface (Finlay and Darlington, 1995; Clark et al., 2001). During evolution a 1,000-fold increase in cortical surface occurred from mouse to human, as opposed to merely an ≈2-fold increase of cortical thickness (Rakic, 1988). To date, little is known about the molecular basis of horizontal expansion of the neuroepithelium (NE), but nuclear β-catenin appears to be a crucial downstream player (Chenn and Walsh, 2002; Falk et al., 2008).

Thymosin β4 (Tβ4) is a highly conserved and abundantly expressed 43 amino acid polypeptide with multiple intra- and extracellular functions. Originally thought to be a thymic hormone, Tβ4 was found to be the major actin sequestering polypeptide in various cell types (Safer et al., 1991). Since the discovery of an autocrine and paracrine proangiogenetic effect of Tβ4 in vitro (Grant et al., 1999), various Tβ4 functions beyond actin sequestering have been discovered, including stem-cell activation (Philp et al., 2004; Smart et al., 2007), promotion of cell survival and migration (Bock-Marquette et al., 2004), as well as enhancement of invasiveness and metastatic

Current address for Hans-Georg Wirsching: Laboratory of Molecular Neuro-Oncology, Department of Neurology, University Hospital Zürich, CH-8008 Zürich, Switzerland.

Grant sponsor: GRK; Grant number: 1104 (to B.B.S.).

*CORRESPONDENCE TO: Beate Brand-Saberi, Ruhr-Universität Bochum, Institut für Anatomie, Abteilung für Anatomie und Molekulare Embryologie, Universitätsstraße 150, Gebäude MA, Ebene 5, Raum 161, D-44801 Bochum, Germany. E-mail: beate.brand-saberi@rub.de

Received May 24, 2010; Revised December 30, 2010; Accepted November 20, 2011
DOI 10.1002/cne.23004
Published online November 25, 2011 in Wiley Online Library (wileyonlinelibrary.com)

potential of cancer cells (Cha et al., 2003; Wang et al., 2004).

It was shown that Tβ4 could promote cadherin downregulation and β-catenin accumulation by activating integrin linked kinase (ILK) and the survival kinase Akt (Wang et al., 2003; Bock-Marquette et al., 2004), thus suggesting a putative role for horizontal expansion of the NE (Chenn and Walsh, 2002; Falk et al., 2008). Moreover, Tβ4 has been suggested to play a role in the macroscopic development of the zebrafish brain by acting as a signaling molecule (Roth et al., 1999), but so far few studies dealt with the implications of Tβ4 in mammalian brain development.

To further elucidate the functions of Tβ4 in brain development, we analyzed the differential expression of Tβ4 during development of the chicken OT and performed in ovo overexpression and shRNA-based knockdown at the onset of tectal development using retroviral transduction and vector-based electroporation.

MATERIALS AND METHODS

Tβ4 overexpression and knockdown

A pDrive vector (Qiagen, Duesseldorf, Germany), previously designed by members of our group (Dathe and Brand-Saberi, 2004), served as a template to obtain the whole coding sequence of *cTβ4* for Tβ4 overexpression. The following primers were used: 5′-GGCTAGCATCGATT CAGGCCACCATGTCCGACAAACCCGA-3′ (upstream) and 5′-GGGATCCGCAGATTTCATTACGATTCACC-3′ (downstream). The obtained fragment was cloned into the enhanced green fluorescent protein (EGFP) coexpressing vector plasmid *pIRES2-EGFP* under the control of the *CMV* promoter (Clontech, Mountain View, CA) for electroporation and into the replication-competent retroviral system *RCAS(BP)A* (Logan and Tabin, 1998). Sequencing confirmed that both vector systems contained the complete open reading frame (ORF) of *cTβ4*, and that the ORF was preceded by the consensus sequence 5′-GCCACC-3′ for binding of the initiator complex (Kozak, 1987).

For Tβ4 knockdown, we designed three vector-based shRNA constructs to target *cTβ4* in the regions of 5′-GAGATCGAGAAATTTGACA-3′, 5′-GCGGGTGAATCGTAAT GAAA-3′, and 5′-GGTGGGACTACAGTAAACTA-3′ sequences of the chicken *Tβ4* primary transcript. Oligo-nucleotides coding for shRNA molecules were produced by Invitrogen (Karlsruhe, Germany) and cloned under the control of the U6 promoter into an EGFP coexpressing vector generated by us (Dai et al., 2005). To enhance knockdown effectiveness, a cocktail of all three plasmids was used for electroporation. The functionality of the respective constructs for Tβ4 overexpression and knockdown was investigated by in situ hybridization.

In ovo electroporation and retroviral transduction

Fertilized chicken eggs (*Gallus domesticus*) were obtained from a local poultry farmer and incubated for 48 or 72 hours. One to 2 ml of albumin was removed from the egg and the top half of the eggshell was cut to create a working window. Solutions containing the effector DNA plasmids for electroporation at a concentration of about 6 ng/μl, or supernatant of RCAS-BP(A) retrovirus transduced 293T cells were supplemented with fast green powder (Sigma-Aldrich, St. Louis, MO). The respective solutions were mouth-pipetted into the second brain vesicle or mesencephalon, respectively. Access was chosen caudally from through the neural tube to prevent damage to the brain. When plasmids were injected, electroporation was carried out with an Electro Square Porator ECM 830 (BTX, Hawthorne, NY) programmed with the following settings: five pulses of 20 ms duration, 27V, and 200 ms intervals. A platinum wire was used for the cathode and a tungsten wire for the anode (both 0.3 mm diameter). Unwanted distribution of the electric field was prohibited by insulating the nonopposing surfaces with nail polish. After 24 hours of reincubation, embryos with EGFP signal but without any electroporation artifacts such as burning or massive deformation were submitted to the next process of experiments, in situ hybridization or immunohistochemistry.

In situ hybridization

A riboprobe targeting Tβ4 mRNA (accession number: NM_001001315) was prepared as previously described (Dathe and Brand-Saberi, 2004). Harvested embryos were fixed overnight at 4°C in 4% paraformaldehyde (PFA) / phosphate-buffered saline (PBS) (pH 7.4), dehydrated in methanol, and stored at −20°C. Whole-mount in situ hybridization was performed as previously described (Nieto et al., 1996). Embryos were frozen and sectioned with a cryotome at 30–35 μm. Expression of Tβ4 at embryonic day (E)7–E21 was investigated in paraffin slices. Sections (10 μm) were mounted onto silanized slides and in situ hybridization was performed as previously described (Rodriguez-Niedenfuhr et al., 2001).

Antibodies

The polyclonal rabbit antiphospho-histone H3 antibody was obtained commercially (Millipore, Temecula, CA, cat. #06-570, lot #0703053576) (Table 1). The manufacturer tested the specificity of this antibody with immunoblot on acid extracts of colcemid-treated and untreated HeLa cells and demonstrated a single band of appropriate molecular weight (17 kD) specifically in the colcemid-treated group. Within the neuroepithelium of control chicken

TABLE 1.
Antibodies Used for Immunohistochemistry

Antigen	Immunogen	Manufacturer, catalog number, species, type	Dilution
Phospho-histone H3	KLH-conjugated peptide (ARK[pS]TGGKAPRKQLC) corresponding to amino acids 7-20 of human Histone H3	Millipore, cat. #06-570, lot #0703053576, rabbit polyclonal	1:100
Doublecortin	KLH-conjugated synthetic peptide (YLPLSLDDSDSLGDSM) corresponding to amino acids 387–402 of human DCX and 346-361 of chicken DCX	Abcam, cat. #ab18723, rabbit polyclonal	1:500
Neuron-specific beta-III tubulin (TuJ1)	Microtubules derived from rat brain	R&D Systems, cat. #MAB1195, lot #HGQ01, mouse monoclonal	1:100
Bromodeoxyuridine (BrdU)	Bromodeoxyuridine-bovine serum albumin concentrate	Millipore, cat. #MAB3424, lot #NG1812620, mouse monoclonal	1:200

optic tecta, staining was almost entirely restricted to nuclei of cells located in the ventricular zone where the pool of mitotic cells, i.e., neural stem and progenitor cells, reside and divide (Gray et al., 1988). Accordingly, the observed staining pattern matched our expectation and we therefore concluded that the antibody crossreacted effectively and was cell type-specific in chicken.

The polyclonal rabbit anti-doublecortin antibody was obtained commercially (Abcam, Cambridge, UK; cat. #ab18723). According to the manufacturer's information, the antibody crossreacts effectively and specifically with chicken doublecortin (DCX) and recognizes a 45-kDa band in western blot on newborn mouse brain tissue lysate. DCX is a migration-associated early neuronal fate marker (Francis et al., 1999; Dellarole and Grilli, 2008). Specificity of this antibody was further confirmed by costaining with a second early neuronal marker, Tuj1 (Fig. 1H–J).

The monoclonal mouse Tuj1 antibody is directed against neuron-specific β-III tubulin and was obtained commercially (R&D Systems, Minneapolis, MN; cat. #MAB1195). On western blot this antibody recognizes the mammalian and chicken neuron-specific class III-tubulin but not other tubulin isotypes in glial cells (manufacturer's technical information). This antibody has been used in the chick optic tectum to stain neuronal bodies in a well-defined morphological pattern that was identical to our observations (Snow and Robson, 1995).

The monoclonal mouse anti-bromodeoxyuridine (BrdU) antibody specifically recognizes proliferating cells in tissues (Schutte et al., 1987; Hayashi et al., 1988) and was obtained commercially (Millipore; cat. #MAB3424, lot #NG1812620). This antibody has been used in the chick optic tectum to stain proliferating cells in a well-defined morphological pattern that was identical to our observations (Schlosshauer et al., 1990).

The following secondary antibodies were used: Cy3-conjugated goat antimouse IgG (1:250, Jackson, West Grove, PA), Cy3-conjugated donkey antirabbit IgG (1:200, Jackson,), FITC-conjugated goat antimouse IgG (1:200, Dianova, Hamburg, Germany), and FITC-conjugated goat antirabbit IgG (1:200, Jackson).

BrdU pulse labeling

Embryos were treated on E4 with 0.2 ml of 40 mM 5-bromo-2′-deoxyuridine (BrdU) solution in PBS (pH 7.4) and reincubated for 30 minutes. After rinsing, the embryos were fixed in a mixture of 3% glacial acid and 97% methanol and then embedded in paraffin.

Immunohistochemistry

Cryosections were washed in PBS and blocked with 0.1M PBS containing 10% lamb serum for 30 minutes. Paraffin sections underwent standard deparaffinization procedures and heat-induced epitope retrieval prior to blocking with 0.1M PBS containing 10% lamb serum for 30 minutes. Then the sections were incubated with the first antibodies diluted in 0.1M PBS containing 10% lamb serum for 24 hours at 4°C. Secondary antibodies were also diluted in 0.1M PBS containing 10% lamb serum and incubation was performed for 90 minutes at room temperature.

Image detection and analysis

Harvested embryos were staged as described (Hamburger and Hamilton, 1951). For convenience, the staging system according to embryonic days was used subsequently. An axioscope (Zeiss, Jena, Germany) was used for image detection. Cy3 or GFP filters, respectively (Zeiss), were used for fluorescence detection. A DC 300F digital camera (Leica, Wetzlar, Germany) was used for documentation. Additionally, images of Figure 1H–J and Figure 7 were obtained using an LSM 510 laser scanning microscope (Zeiss). Slight modifications of the contrast and brightness settings and occasional adjustment of

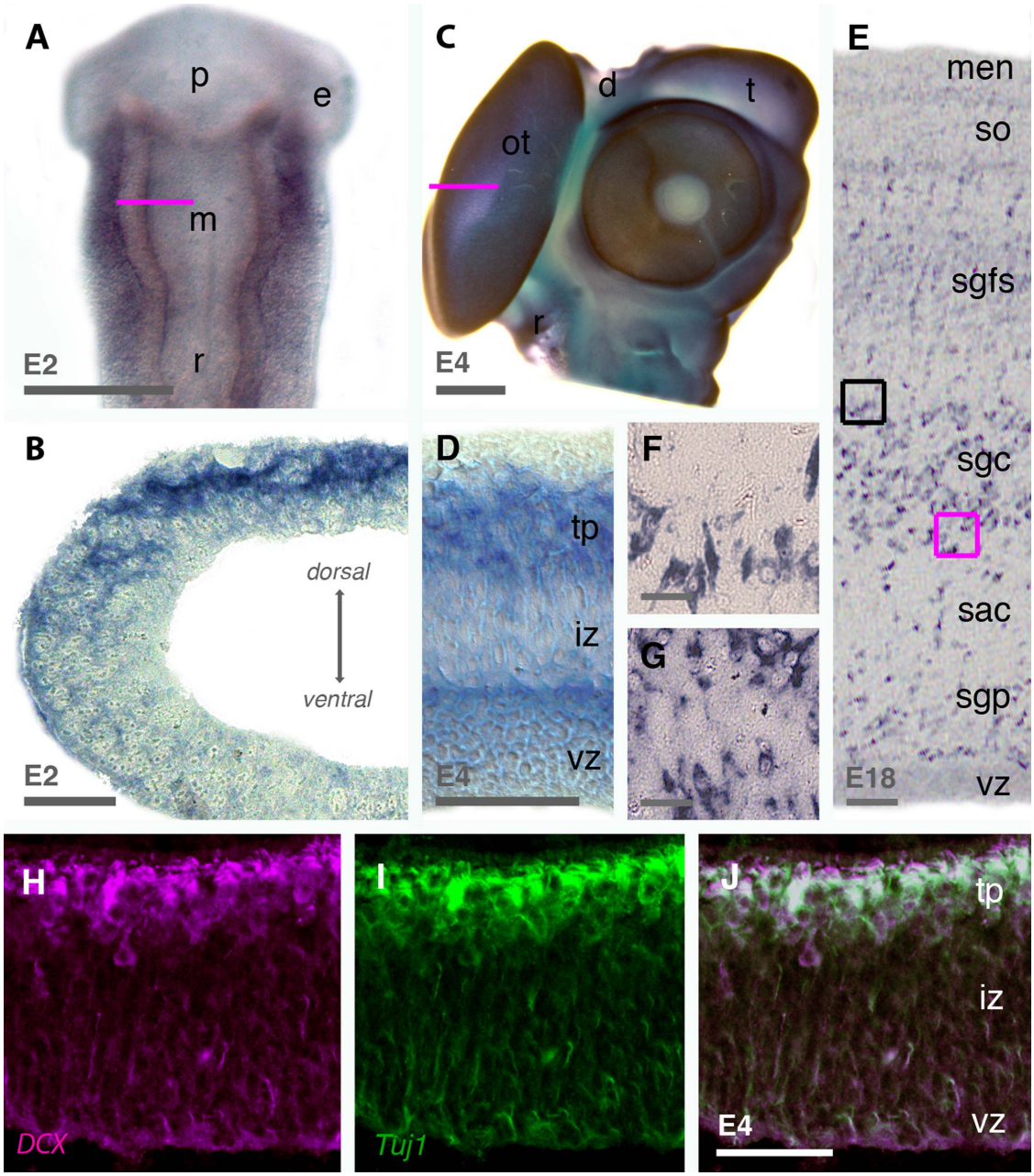

Figure 1. Tβ4 expression during development of the OT. Tβ4 in situ hybridization (A–G) and immunohistochemistry of early neuronal markers DCX and Tuj1 (H–J). **A:** Whole-mount preparation on E2, dorsal view. **B:** Coronary section as indicated by magenta bar in panel A. **C:** Lateral view of whole-mount head on E4. **D:** Section as indicated by magenta bar in panel C. **E:** Coronary section on E18. **F,G:** magnifications as indicated by black square (F) and magenta square (G) in panel E. **H–J:** DCX (H), Tuj1 (I), overlay (J). p, prosencephalon; m, mesencephalon; r, rhombencephalon; e, eye; ot, optic tectum; d, diencephalon; t, telencephalon; tp, tectal plate; iz, intermediate zone; vz, ventricular zone; men, pia mater; so, stratum opticum; sgfs, stratum granulosum et fibrosum superficiale; sgc, stratum griseum centrale; sac, stratum album centrale; sgp; stratum granulosum periventriculare. Scale bars = 500 μm in A,C; 100 μm in B,D,E; 20 μm in F,G; 40 μm in H–J. [Color figure can be viewed in the online issue, which is available at wileyonlinelibrary.com.]

backgrounds were made using Adobe Photoshop 7.0 (Adobe Systems, San Jose, CA). For statistical analysis, H3P+ and BrdU+ cells were counted as indicated, corrected for cell size by using the Abercrombie factor (Guillery, 2002), and subjected to one-way analysis of variance (ANOVA) using GraphPad Prism software (La Jolla, CA).

RESULTS

Developmental expression of Tβ4 in the chicken optic tectum

The expression pattern of Tβ4 during chicken development, including a rough overview of its expression in the developing brain, has been reported previously (Dathe and Brand-Saberi, 2004). As a basis for investigating

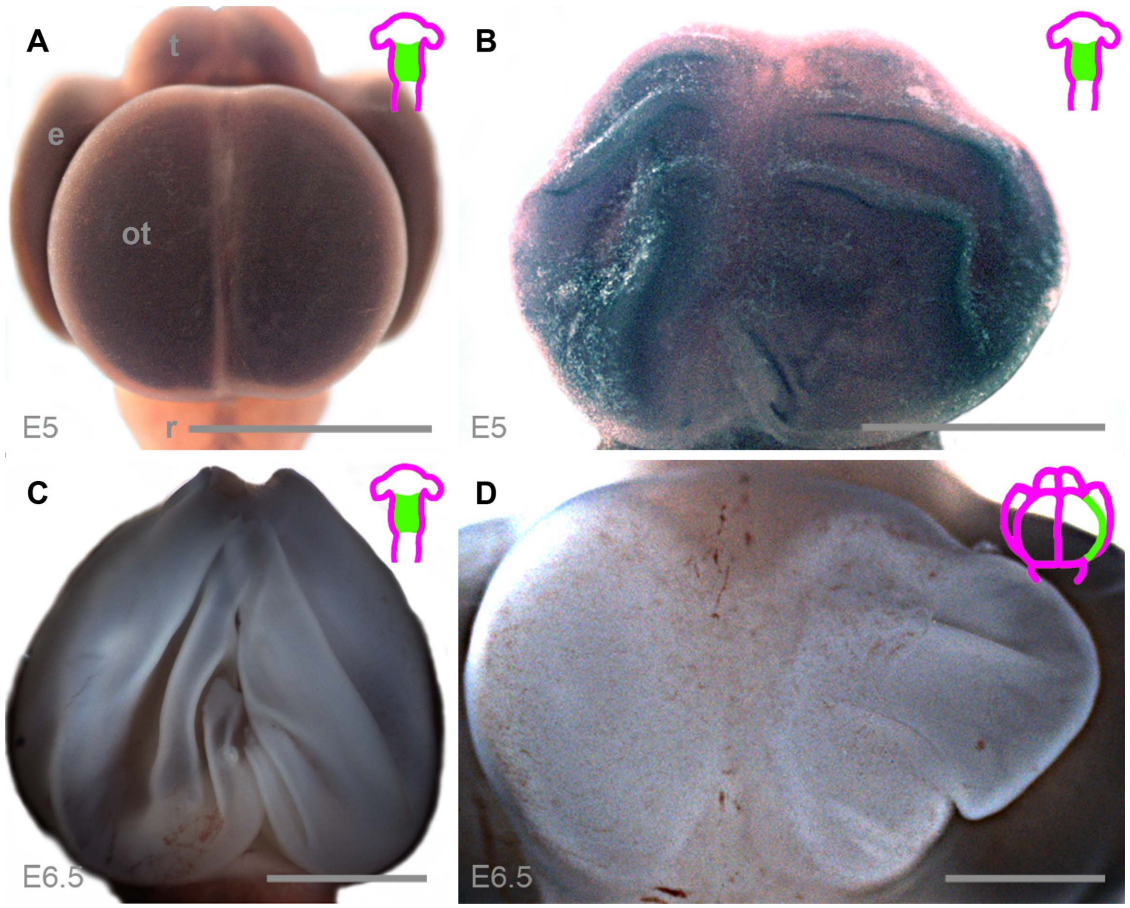

Figure 2. Retroviral overexpression of Tβ4 causes enlargement and folding of the OT. Dorsal views of optic tecta in whole mount heads after in situ hybridization (A,B) and unstained (C,D). Icons: Sites of *RCAS* injections on E2 (A–C) or E3.5 (D) are marked green. **A,B:** E5, 72 hours of reincubation after intraluminar injection of an empty *RCAS* for control (A) and *RCAS-Tβ4* for overexpression of Tβ4 (B). Diffuse Tβ4 overexpression led to enlargement and folding of the OT. **C:** E6.5, 4.5 days of reincubation after intraluminar injection of *RCAS-Tβ4*. Surrounding mesenchymal tissue has been removed to reveal folding of the NE. **D:** E6.5, 72 hours of reincubation after unilateral injections of *RCAS-Tβ4* into the right tectal hemisphere. Only the manipulated hemisphere is enlarged and folded. e, eye; t, telencephalon; ot, optic tectum; r, rhombencephalon. Scale bars = 1,000 μm. [Color figure can be viewed in the online issue, which is available at wileyonlinelibrary.com.]

functions of Tβ4, we first sought to characterize the pattern of normal Tβ4 expression in the developing OT. At the onset of OT development around E2 the tectal NE consists mostly of neural stem cells (NSC) and some neural progenitor cells (NPCs) (Gray et al., 1988). NPCs are generated by asymmetric division of NSCs and, together, NSCs and NPCs constitute the pool of proliferating cells during brain development. Early expansion of this cell population is thought to be the major mechanism that regulates growth of the developing brain (Chenn and Walsh, 2002; Kingsbury et al., 2003; Falk et al., 2008).

On E2, in situ hybridization revealed marked expression of Tβ4 in the paraxial mesoderm adjacent to the early mesencephalon (Fig. 1A). Within the mesencephalon of E2 embryos, predominant Tβ4 expression was found dorsally in the early OT (Fig. 1B).

Neurogenesis, i.e., the generation of postmitotic neurons by asymmetrical division of NPCs, begins around E3 within the tectal NE (Gray et al., 1988). Particularly strong staining for Tβ4 mRNA was found in the OT after the onset of neurogenesis, on E3–E5 (Fig. 1C). During these stages surface expansion of the OT proceeds markedly faster than in the other brain structures.

Until E4, proliferation of NPCs gave rise to a population of postmitotic neurons that line up radially and form the tectal plate (Gray et al., 1988; Gray and Sanes, 1991). Immunohistochemistry with the neuronal differentiation markers DCX and Tuj1 show a near identical staining pattern for both markers and outline the tectal plate on E4 (Fig. 1H–J). Comparison of the expression patterns of DCX and Tuj1 to Tβ4 mRNA expression in matched slices confirmed the localization of Tβ4-expressing cells to the tectal plate (Fig. 1D). On E4, we further found strong staining of Tβ4 mRNA in a second, thin layer adjacent to the VZ, where postmitotic cells halt briefly before migrating through an intermediary zone toward the basally located tectal plate (Fig. 1D).

The onset of radial migration of postmitotic neurons along radial glia processes begins in the OT around E7 and is the developmental basis of the typical tectal layering found in the adult OT (Gray and Sanes, 1991). On E7–E21, cells in these layers are strongly stained for Tβ4 mRNA (Fig. 1E). These Tβ4-positive cells exhibit a polarized phenotype reminiscent of migratory activity and/or neurite outgrowth (Fig. 1F,G). Of note, the VZ stains only weakly or not at all for Tβ4 mRNA throughout tectal development.

Tβ4 regulates growth of the tectal hemispheres

To further elucidate Tβ4 functions in OT development, we used in ovo retroviral transduction and plasmid electroporation for Tβ4 overexpression and Tβ4 knockdown.

First, we injected an *RCAS-Tβ4* retrovirus for stable Tβ4 overexpression directly into the lumen of the mesencephalon on E2. Overexpression was confirmed by in situ hybridization and controls were performed with empty *RCAS*. Control virus had no effect on macroscopic development (Fig. 2A), whereas Tβ4 overexpression led to asymmetry, enlargement, and folding of the entire mesencephalon within 3–5 days (Fig. 2B–D). The duration of reincubation was limited by deadly hemorrhage. Whole-mount in situ hybridization revealed Tβ4 overexpression throughout the entire OT (Fig. 2B).

Injection of *RCAS-Tβ4* into single mesencephalic hemispheres allowed comparison between the injected hemisphere with the not manipulated hemisphere in the same embryo (Fig. 2D). The same macroscopic alterations stemming from the pan-mesencephalic Tβ4 overexpression was spatially restricted to the manipulated hemisphere.

Unilateral electroporation of EGFP coexpressing plasmids for Tβ4 overexpression or knockdown allowed more precise localization of manipulated cells. Control electroporation of an empty *pEGFP* vector plasmid had no effect on macroscopic development and EGFP expression levels decreased from ventral to dorsal, thus reflecting the ventrodorsal direction of horizontal expansion of the tectal NE (Fig. 3A). As horizontal expansion of the NE is the result of symmetric NSC divisions, plasmid and EGFP load decrease along a gradient following the direction of growth.

A similar EGFP gradient was found after electroporation of plasmids coding for Tβ4-targeting shRNA (*pEGFP-shTβ4*), although on a smaller scale due to decreased growth of Tβ4-depleted hemispheres (Fig. 3B). Electroporation of *pEGFP-Tβ4* for Tβ4 overexpression led to the identical macroscopic findings as those observed after *RCAS-Tβ4* transduction, including enhanced growth and folding (Fig. 3C,D). In contrast to controls, the EGFP signal of Tβ4 overexpressers was located predominantly at the dorsal edge of the OT (Fig. 3C,D).

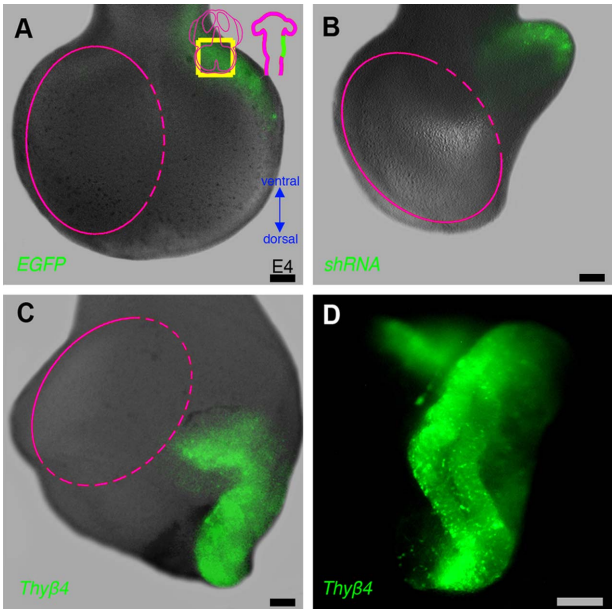

Figure 3. Tβ4 expression regulates growth of tectal hemispheres. Optic tecta 48 hours after unilateral electroporation of EGFP coexpressing vector plasmids. A–C: Rostral views, UV-fluorescence merged images. D: 2× enlarged dorsal view of C, fluorescent image. Left icon: Scheme drawing of an E4 chicken brain, rostral view. The yellow square represents the displayed panel. Right icon: Site of electroporation on E2. Magenta ellipses: estimated margins of the nonelectroporated hemisphere. Dotted lines: transition to electroporated hemisphere. **A:** Control electroporation of empty vector has no macroscopic morphological effect. The expression level of EGFP decreases from ventral to dorsal. **B:** Tβ4 knockdown impairs growth of the electroporated hemisphere and induces deviation of the interhemispheric midline toward the manipulated hemisphere. EGFP expression is restricted to a small area. **C,D:** Tβ4 overexpression led to development of a folded excrescence; EGFP detection was stronger and located further dorsally, as compared with control or shRNA electroporation. EGFP-negative areas of the OT are enlarged as well. Scale bars = 100 μm. [Color figure can be viewed in the online issue, which is available at wileyonlinelibrary.com.]

We conclude that differential Tβ4 expression is a required factor for growth of the OT and that differential Tβ4 expression can result in development of neuroepithelial folds resembling gyri and sulci of higher mammals.

Histomorphological alterations due to Tβ4 overexpression and knockdown

To estimate the extent of altered growth patterns of Tβ4 overexpressing or Tβ4 depleted hemispheres, we quantified the number folds in respectively distorted embryos (Fig. 4A). We observed folding of the NE due to Tβ4 overexpression in the optic tecta of eight embryos. In five of these cases, Tβ4 overexpression was performed by transduction with an *RCAS-TB4* retrovirus and in three

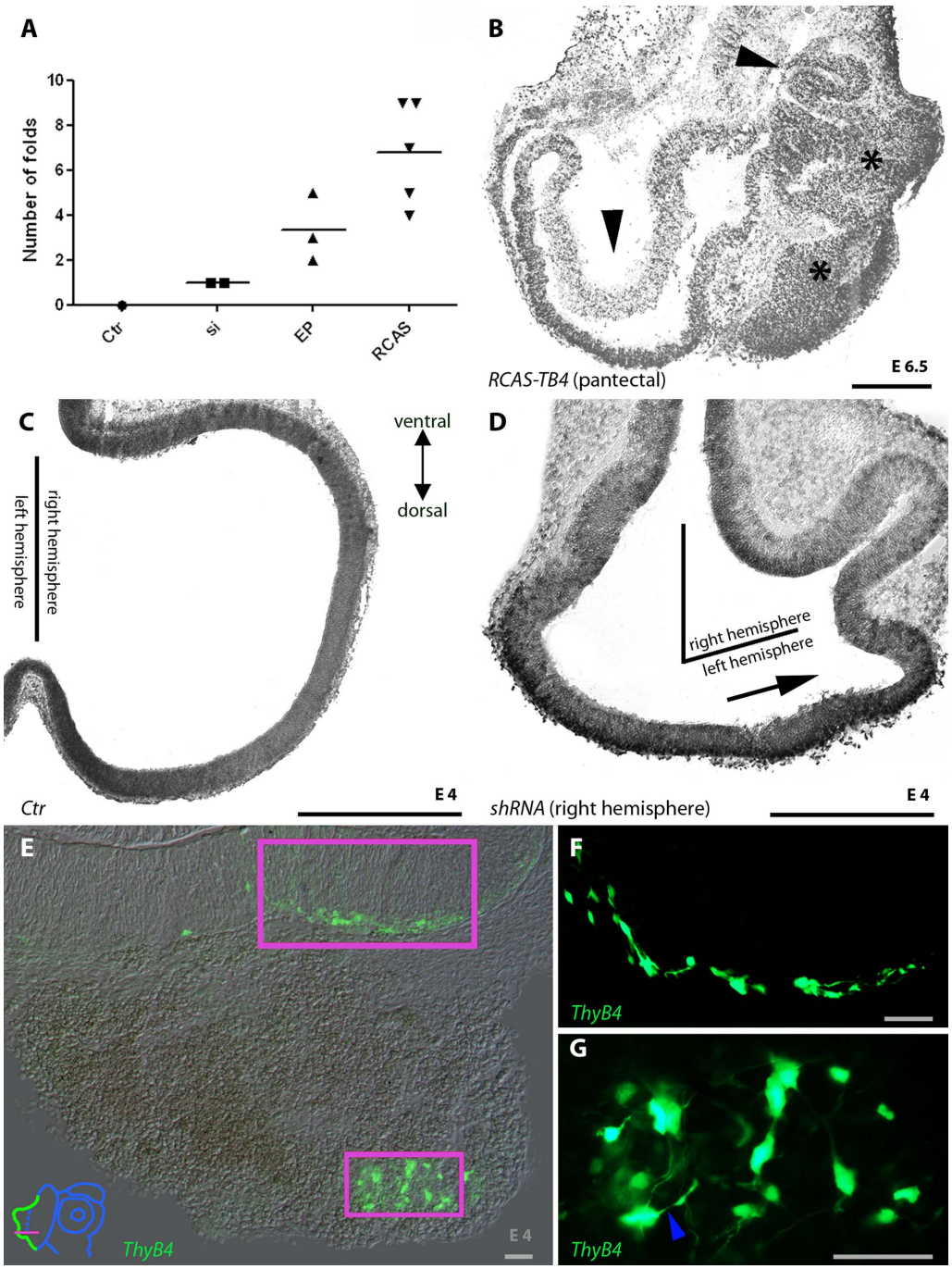

Figure 4. Histomorphological alterations due to Tβ4 overexpression and knockdown. **A:** Overview of optic tecta that showed a folded phenotype due to altered TB4 expression. No folding was observed in controls. Ctr, control; si, Tβ4 knockdown; EP, Tβ4 overexpression by electroporation; *RCAS*, Tβ4 overexpression by retroviral transduction. **B:** E6.5, 4.5 days after viral transduction for Tβ4 overexpression. Black arrowheads indicate neuroepithelial folding; asterisks indicate disruption of the epithelial structure. **C,D:** E4, 48 hours after unilateral electroporation of vector plasmids for control (C) or Tβ4 knockdown (D). Unilateral Tβ4 depletion in the right hemisphere leads to decreased growth and shifting of the midline axis due to overgrowth of the unmanipulated left hemisphere (D). The black arrow indicates the growth direction of the unmanipulated hemisphere. **E:** E4, 48 hours after unilateral electroporation of an EGFP coexpressing vector plasmid for overexpression of Tβ4. Slice preparation of a tectal excrescence and adjacent neuroepithelium as indicated by the magenta bar (icon). Tissue arrangement within the excrescence is fundamentally different from neuroepithelium (NE) and adjacent stroma (ST). EGFP-positive cells are located dorsally within excrescences and at the subpial surface of the neuroepithelium. **F,G:** Fluorescent magnifications as indicated by the magenta rectangles in E. Tβ4 overexpressing cells form tangentially oriented files (F). The soma and a swelling within a long cytoplasmic process are interconnected by a thin cytoplasmic bridge (blue arrowhead). Scale bars = 500 μm in B–D; 100 μm in E; 40 μm in F; 20 μm in G. [Color figure can be viewed in the online issue, which is available at wileyonlinelibrary.com.]

TABLE 2.
Overview of Analyzed Optic Tecta

Method	*N*	Asymmetry	Decrease	Increase	Folding
RCAS il overex	24	14 (58.3%)	0	12 (50.0%)	3 (21.4%)
RCAS il control	18	2 (11.1%)	0	0	0
RCAS ic overex	17	8 (47.1%)	1 (5.9%)	7 (41.2%)	2 (25%)
RCAS ic control	19	1 (5.3%)	0	0	0
EP overex	13	11 (84.6)	0	11 (84.6%)	3 (27.3%)
EP knockdown	16	11 (68.8%)	11 (68.8%)	0	2 (18.2%)
EP control	17	1 (5.7%)	0	1 (5.7%)	0

Decrease and increase were only considered if the respective hemispheres were altered in tangential diameter by 30% or more, as compared with their nonmanipulated counterpart or control transduced brains, respectively. il, intraluminal injection; ie, intraepithelial injection; EP, electroporation.

cases using electroporation of *pEGFP-TB4*. Of note, decreased growth due to electroporation of *pEGFP-shTB4* led to folding of the tectal hemisphere in two cases as well. However, the mechanism appears to be different from folding due to Tβ4 overexpression, as discussed below. An overview of all manipulated embryos is provided in Table 2.

To further elucidate effects of Tβ4 gain- and loss-of-function, we investigated histomorphological characteristics of folded OTs in tangential cross-sections.

In OTs where Tβ4 overexpression had led to folding of the NE, space-consuming growth restricted ventricular lumina (Fig. 4B). Moreover, opposing ventricular surfaces in NE folds tended to melt (Figs. 4B, 5C). In extreme cases ($n = 5$), macroscopically observed excrescences lost their epithelial polarity entirely and melted with the surrounding stroma at the pial surface (Figs. 4B,E, 5C). Interestingly, only a subset of the cells that constituted the heteromorphic mesenchymal masses of such nonepithelial excrescences in *pEGFP-Tβ4* electroporated OTs exerted a detectable EGFP signal indicative of Tβ4 overexpression (Fig. 4E,G). Within the intact NE, Tβ4 overexpressing cells aligned to the pial surface of the NE in a tangential orientation (Fig. 4F).

In contrast, electroporation of *pEGFP* or *pEGFP-shTβ4* did not compromise the epithelial structure of the OT (Fig. 5A,B). EGFP-positive cells were scattered throughout the layers of the NE, reflecting the normal distribution of different cell populations that had been randomly transformed (Fig. 5D,E).

However, in cases of strong inhibition of growth due to Tβ4 knockdown, growth of manipulated hemispheres could be almost entirely abrogated, while growth of contralateral, unmanipulated hemispheres was not inhibited (Fig. 4D). Accordingly, unmanipulated hemispheres grew relatively stronger than Tβ4-depleted hemispheres, which induced a shift of the interhemispheric midline axis (Figs. 3B, 4D, 5B). In extreme cases ($n = 2$), this led to an overgrowth of the Tβ4-depleted hemisphere by the unmanipulated contralateral hemisphere and consecutively to the occurrence of the growth-inhibited hemisphere as an NE "fold" with decreased ventricular lumen (Figs. 4D, 5B). Of note, this "folding" occurred in a preformed localization, i.e., the ventricular lumen of the Tβ4-depleted hemisphere and multiple folds did not occur due to Tβ4 knockdown (Fig. 4A,D). Furthermore, Tβ4-depleted hemispheres did not appear thinner or otherwise structurally weaker than unmanipulated hemispheres.

Tβ4 overexpression promotes proliferation

Virus and plasmids for Tβ4 overexpression or knockdown were introduced from the luminal side of the neuroepithelium into the early mesencephalon on E2. At this time, the mesencephalon consists mostly of proliferative cells, since neurogenesis does not start until about E3 (Gray et al., 1988).

Immunohistochemical staining for the metaphase marker phosphorylated histone H3 (H3P) revealed regulatory effects of Tβ4 expression on the number of mitotic cells: Overexpression of Tβ4 was followed by a significantly increased detection of H3P+ cells as compared with controls and there was a tendency of decreased detection of H3P+ cells due to Tβ4 knockdown (Figs. 5, 6). Tangential orientation of sections to the ventricular surface was excluded by comparison with stacks of slices through the whole OT and accordingly central slices were chosen for further analysis. Since distortion due to differential growth and folding made matching of cross-sections critical, we further matched slices with similar H3P expression levels of the unmanipulated NE to exclude a confounding error due to rostrocaudal gradients of cell division (LaVail and Cowan, 1971).

To exclude that enhanced H3P staining in Tβ4 overexpressing tissue was due to cell cycle arrest, we furthermore performed BrdU pulse labeling (Fig. 7). Enhanced BrdU uptake in Tβ4-overexpressing tissue compared with unmanipulated, matched control hemispheres in the same embryos confirmed that Tβ4 overexpression significantly enhanced proliferation (Figs. 5L, 6F).

DISCUSSION

The aim of the present study was to investigate putative functions of Tβ4 in the development of the chicken

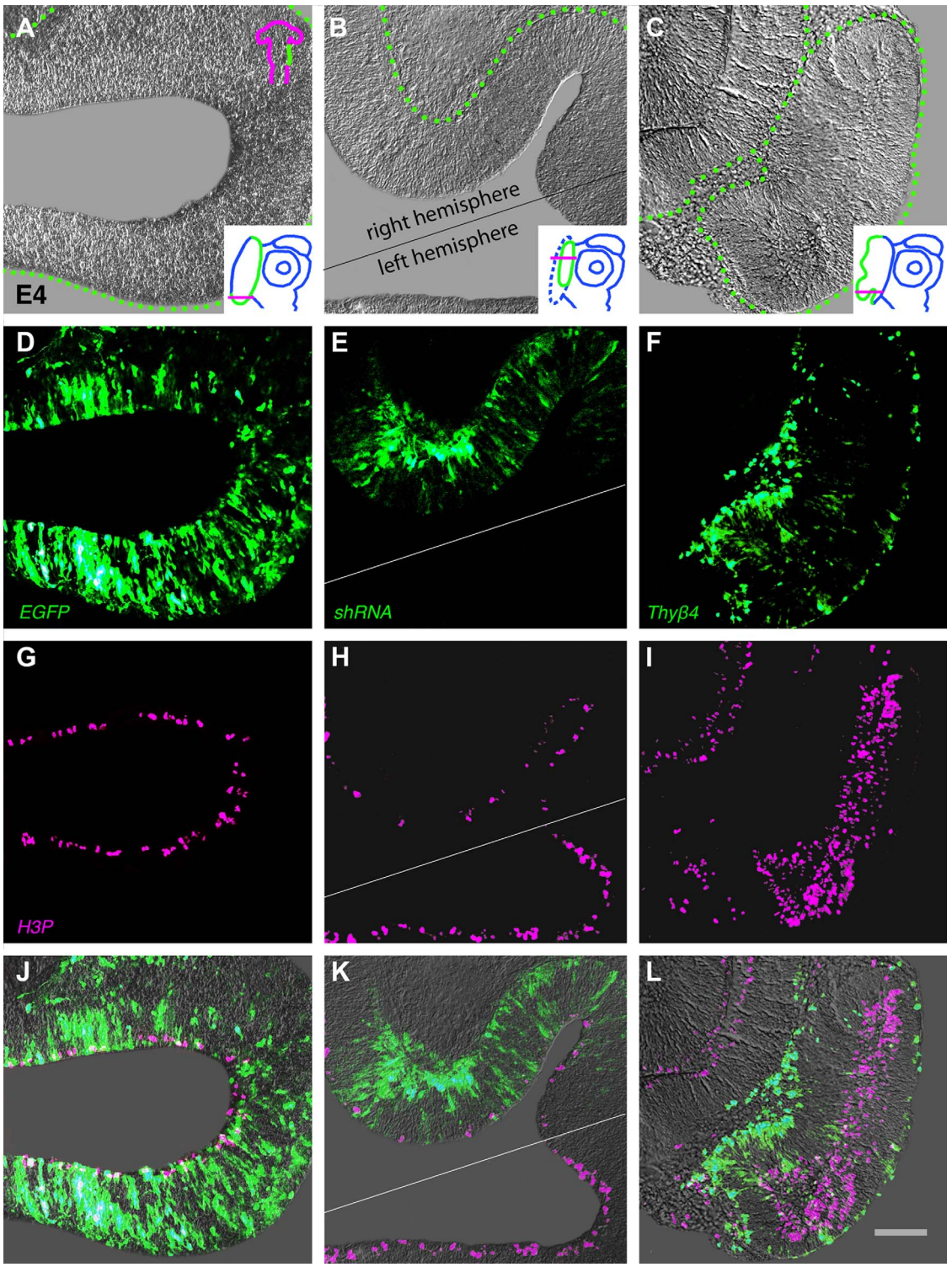

Figure 5. Tβ4 expression regulates the number of mitotic cells in the ventricular zone. E4, optic tecta 48 hours after unilateral electroporation of *EGFP* expressing vector plasmids on E2 (top icon in A). Control (left), Tβ4 knockdown (center) and Tβ4 overexpression (right). Horizontal slices as indicated by magenta bars (bottom icons in **A–C**). Left: electroporation of empty *EGFP* **(D)** yields no macroscopic effect (A) and has no influence on H3P expression in the vz **(G,J)**. Center: Tβ4 knockdown **(E)** inhibited growth of the manipulated hemisphere which was subsequently overgrown by the nonmanipulated tissue of the contralateral side (B). The shifted interhemisphere axis has been estimated according to the respective whole-mount preparation (gray line). Fewere H3P-immunopositive cells were detectable in the ventricular zone in EGFP+ areas **(H,K)**. Right: Tβ4 overexpression **(F)** led to the development of an excrescence, which had partially lost its epithelial structure (C). H3P detection was increased and occurred in ectopic localization, i.e., within the excrescences **(I)**. Mitotic cells and Tβ4 overexpressing cells constituted two widely separate cell populations **(L)**. vz, ventricular zone; iz, intermediate zone; tp, tectal plate. Dotted lines in A–C: Basal neuroepithelial margins. Scale bar = 100 μm. [Color figure can be viewed in the online issue, which is available at wileyonlinelibrary.com.]

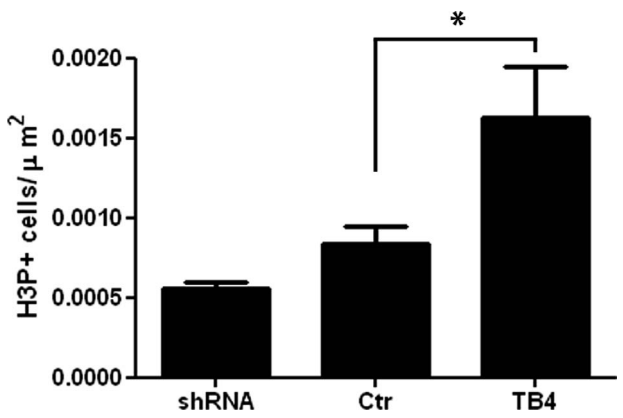

Figure 6. Tβ4 expression levels correlate with numbers of H3P-positive cells. OT were electroporated on E2 with *pEGFP* for control ($n = 5$, *Ctr*), *pEGFP-shTβ4* for knockdown of Tβ4 ($n = 2$, *shRNA*) and *pEGFP-Tβ4* for overexpression of Tβ4 ($n = 2$, *TB4*). The numbers of H3P-positive cells were counted within EGFP expressing hemispheres on E3. $^*P < 0.03$.

OT. Therefore, we first delineated normal Tβ4 expression in the OT of wildtype (WT) chicken embryos. We found vast numbers of Tβ4-positive cells in all neuronal layers throughout tectal development, but not within the VZ where neural stem cells reside and divide (Fig. 1). Tβ4 staining colocalized with the neuronal markers Tuj1 and DCX in matched slices and Tβ4-positive cells exhibited morphological features of neurons, including neurites and characteristic cell body shapes. Tβ4 expression was also found in a thin layer adjacent to the VZ, where postmitotic cells halt briefly before migrating toward the tectal plate (Fig. 1D). These observations support previous reports of Tβ4 expression in neurons of the developing central nervous system (Roth et al., 1999) and of in vitro data that have suggested a role for Tβ4 in neuronal differentiation (Border et al., 1993; Yang et al., 2008; Mollinari et al., 2009).

To further elucidate Tβ4 functions in tectal development, we performed vector-based overexpression and knockdown studies. We chose a developmental timepoint for manipulation briefly before the onset of neuronal birth (Snow and Robson, 1995). The respective period is characterized by the expansion of the proliferating population and tectal surface (Gray et al., 1988). We found a strong impact of Tβ4 on regulating the growth of the tectal hemispheres (Figs. 2, 3). Tβ4 overexpression led to the production of folds, resembling gyri and sulci in the brains of higher mammals, while Tβ4 knockdown inhibited growth effectively. Surprisingly, in two cases Tβ4 knockdown led to a folded phenotype as well (Fig. 4A,D), which we attributed to an overgrowth by the relatively stronger growing contralateral, unmanipulated hemisphere. This finding contributes to the notion that not only enhanced growth, but in particular differential growth may be the developmental basis of neuroepithelial folding in higher mammals. However, respective experiments in mammals need to be performed to further elucidate the complex mechanisms underlying the massive expansion of the cortical surface during the evolution of higher mammals.

While Tβ4 knockdown did not disrupt the epithelial architecture, the ventricular surfaces of neuroepithelial excrescences that were induced by Tβ4 overexpression tended to melt and the pial surface often dissolved entirely, such that Tβ4 overexpressing cells were intermingled with mesenchymal cells (Figs. 4C,E, 5L). This finding was highly suggestive of a epithelial-to-mesenchymal transition, but in vitro transdifferentiation studies need to be done to confirm this morphological finding. Of note, only a small fraction of cells in mesenchymal excrescences were EGFP+ Tβ4 overexpressing cells, suggesting that a putative tissue transformation could have been induced in a noncell autonomous manner.

In accordance with the developmental expression pattern of Tβ4 in the OT of WT animals (Fig. 1), Tβ4 overexpressing cells aligned to the pial surface of the intact NE and exhibited morphological characteristics of neuronal differentiation. These included neurite outgrowth and extended, often branching cytoplasmic processes with swellings at a distance of 10–30 μm from the soma that were reminiscent of tangentially migrating neurons (Fig. 4F,G) (Marin and Rubenstein, 2001; Martini et al., 2009). Of note, these observations were made on E4, but in WT embryos it is normally not until E6–7 that a minor population of cells form a first migratory stream along the axon fascicles in mediolaterally directed files (Gray and Sanes, 1991). However, we did not perform experiments to directly assess differentiation or cell migration and feel that more research needs to be done to clarify a putative involvement of Tβ4 in differentiation and migration during tectal development.

Staining for the mitosis marker H3P revealed a reduced number of M-phase cells in areas of the NE that were electroporated with *pEGFP-shTβ4* for Tβ4 knockdown, and a vast increase in M-phase cells as a result of Tβ4 overexpression. However, almost no H3P staining was detected in EGFP coexpressing Tβ4 overexpressing cells after electroporation of *pEGFP-Tβ4*, thus indicating that Tβ4 overexpressing cells did not enter M-phase. BrdU pulse labeling confirmed that only a few Tβ4 overexpressing cells proliferated (Fig. 7). Since the overall number of BrdU and H3P-positive cells was increased due to Tβ4 overexpression, we conclude that Tβ4 overexpression expanded and/or activated the proliferating population.

In the past 5 years, increasing evidence has occurred for noncell autonomous regulation of the proliferating population (Yoshimatsu et al., 2006; Falk et al., 2008;

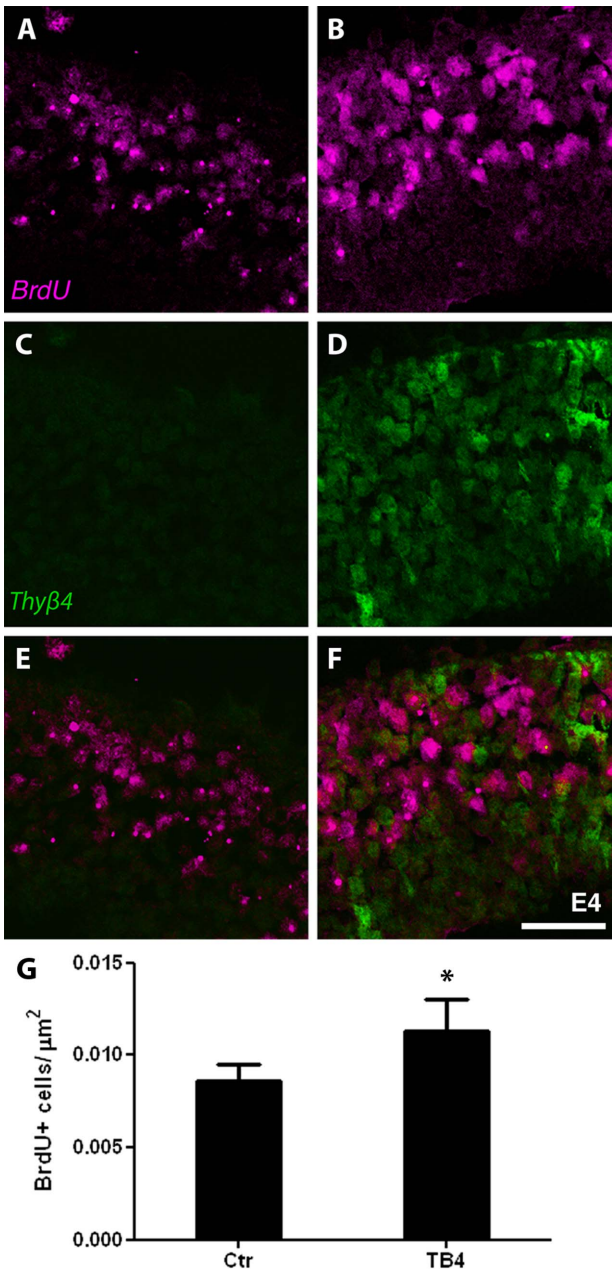

Figure 7. Tβ4 overexpression enhances proliferation. E4, 48 hours after unilateral electroporation of *pEGFP-Tβ4* for Tβ4 overexpression and BrdU pulse labeling. Left: Unmanipulated control hemisphere. Right: Tβ4 overexpressing hemisphere of the same transversal cross-section. **A,B:** BrdU labeling was enhanced in the Tβ4-overexpressing hemisphere. **C,D:** No EGFP expression was detected in unmanipulated hemispheres (C), while EGFP marks electroporated, Tβ4-overexpressing cells (D). **E,F:** overlay; proliferating BrdU-positive cells and Tβ4-overexpressing EGFP-positive cells constituted two widely separate cell populations. Scale bar = 50 µm. *$P < 0.001$. [Color figure can be viewed in the online issue, which is available at wileyonlinelibrary.com.]

Lavado et al., 2010; Aguirre et al., 2010). Because we found only a minor overlap of Tβ4 overexpression and expression of proliferation markers H3P and BrdU (Figs. 5, 7), we suggest that the effects of Tβ4 overexpression on the proliferating population may involve noncell autonomous mechanisms. Furthermore, we suggest that in WT animals the strongly Tβ4-expressing cell population adjacent to the VZ (Fig. 1D) could be involved in a noncell autonomous regulation of the proliferating population under WT conditions.

Studies in mice demonstrated induction of neuroepithelial folds as a result of an expansion of the proliferating population via differential wnt, TGFβ, or lateral periaqueductal (LPA) signaling (Chenn and Walsh, 2002; Kingsbury et al., 2003; Falk et al., 2008). A paracrine role for Tβ4 in stem cell activation and self renewal via ILK activation and consecutively enhanced downstream wnt signaling has been demonstrated in the developing heart of mice (Bock-Marquette et al., 2004; Smart et al., 2007). Although interpreting data generated in the cardiovascular system for brain development is problematic, it should be noted that knockout of ILK is an underlying condition in the pathogenesis of cobblestone lissencephaly (Niewmierzycka et al., 2005), a genetic neurological condition that is characterized by the absence of cortical convolutions.

Downstream effects of ILK signaling furthermore include disruption of caspase-3 activity (McDonald et al., 2008). Considering the similar tissue phenotype between Tβ4 overexpression and caspase-3 and caspase-9 knockout animals (Kuida et al., 1996; Kuida et al., 1998; Cowan and Roskams, 2004), inhibition of apoptosis within the proliferating population seems a viable mechanism that may have contributed to Tβ4-induced cerebral malformation.

In summary, we found that due to its multiple cell autonomous and possibly noncell autonomous effects on proliferation, Tβ4 expression has a large impact on neuroepithelial development. Considering that disruption of tissue architecture and uncontrolled proliferation are also hallmarks of cancer (Hanahan and Weinberg, 2000), we conclude that our results might also indicate a role for Tβ4 in brain tumor biology.

ACKNOWLEDGMENTS

We thank Michael Frotscher for critically reviewing the article, Fangping Dai for preparation of Tβ4 overexpression and knockdown tools, Ulrike Pein, Susanna Glaser, and Ellen Gimbel for technical assistance, and Mushfika Ahmad for reading the article.

LITERATURE CITED

Aguirre A, Rubio ME, Gallo V. 2010. Notch and EGFR pathway interaction regulates neural stem cell number and self-renewal. Nature 467:323–327.

Bock-Marquette I, Saxena A, White MD, Dimaio JM, Srivastava D. 2004. Thymosin beta4 activates integrin-linked kinase

and promotes cardiac cell migration, survival and cardiac repair. Nature 432:466–472.
Border BG, Lin SC, Griffin WS, Pardue S, Morrison-Bogorad M. 1993. Alterations in actin-binding beta-thymosin expression accompany neuronal differentiation and migration in rat cerebellum. J Neurochem 61:2104–2114.
Cha HJ, Jeong MJ, Kleinman HK. 2003. Role of thymosin beta4 in tumor metastasis and angiogenesis. J Natl Cancer Inst 95:1674–1680.
Chenn A, Walsh CA. 2002. Regulation of cerebral cortical size by control of cell cycle exit in neural precursors. Science 297:365–369.
Clark DA, Mitra PP, Wang SS. 2001. Scalable architecture in mammalian brains. Nature 411:189–193.
Cowan CM, Roskams AJ. 2004. Caspase-3 and caspase-9 mediate developmental apoptosis in the mouse olfactory system. J Comp Neurol 474:136–148.
Dai F, Yusuf F, Farjah GH, Brand-Saberi B. 2005. RNAi-induced targeted silencing of developmental control genes during chicken embryogenesis. Dev Biol 285:80–90.
Dathe V, Brand-Saberi B. 2004. Expression of thymosin beta4 during chick development. Anat Embryol 208:27–32.
Dellarole A, Grilli M. 2008. Adult dorsal root ganglia sensory neurons express the early neuronal fate marker doublecortin. J Comp Neurol 511:318–328.
Falk S, Wurdak H, Ittner LM, Ille F, Sumara G, Schmid MT, Draganova K, Lang KS, Paratore C, Leveen P, Suter U, Karlsson S, Born W, Ricci R, Gotz M, Sommer L. 2008. Brain area-specific effect of TGF-beta signaling on Wnt-dependent neural stem cell expansion. Cell Stem Cell 2:472–483.
Finlay BL, Darlington RB. 1995. Linked regularities in the development and evolution of mammalian brains. Science 268:1578–1584.
Francis F, Koulakoff A, Boucher D, Chafey P, Schaar B, Vinet MC, Friocourt G, McDonnell N, Reiner O, Kahn A, McConnell SK, Berwald-Netter Y, Denoulet P, Chelly J. 1999. Doublecortin is a developmentally regulated, microtubule-associated protein expressed in migrating and differentiating neurons. Neuron 23:247–256.
Grant DS, Rose W, Yaen C, Goldstein A, Martinez J, Kleinman H. 1999. Thymosin beta4 enhances endothelial cell differentiation and angiogenesis. Angiogenesis 3:125–135.
Gray GE, Sanes JR. 1991. Migratory paths and phenotypic choices of clonally related cells in the avian optic tectum. Neuron 6:211–225.
Gray GE, Sanes JR. 1992. Lineage of radial glia in the chicken optic tectum. Development 114:271–283.
Gray GE, Glover JC, Majors J, Sanes JR. 1988. Radial arrangement of clonally related cells in the chicken optic tectum: lineage analysis with a recombinant retrovirus. Proc Natl Acad Sci U S A 85:7356–7360.
Gray GE, Leber SM, Sanes JR. 1990. Migratory patterns of clonally related cells in the developing central nervous system. Experientia 46:929–940.
Guillery RW. 2002. On counting and counting errors. J Comp Neurol 447:1–7.
Hamburger V, Hamilton H. 1951. A series of normal stages in the development of the chick embryo. J Morphol 88: 49–92.
Hanahan D, Weinberg RA. 2000. The hallmarks of cancer. Cell 100:57–70.
Hayashi Y, Koike M, Matsutani M, Hoshino T. 1988. Effects of fixation time and enzymatic digestion on immunohistochemical demonstration of bromodeoxyuridine in formalin-fixed, paraffin-embedded tissue. J Histochem Cytochem 36:511–514.
Kingsbury MA, Rehen SK, Contos JJ, Higgins CM, Chun J. 2003. Non-proliferative effects of lysophosphatidic acid enhance cortical growth and folding. Nat Neurosci 6: 1292–1299.
Kozak M. 1987. At least six nucleotides preceding the AUG initiator codon enhance translation in mammalian cells. J Mol Biol 196:947–950.
Kuida K, Zheng TS, Na S, Kuan C, Yang D, Karasuyama H, Rakic P, Flavell RA. 1996. Decreased apoptosis in the brain and premature lethality in CPP32-deficient mice. Nature 384:368–372.
Kuida K, Haydar TF, Kuan CY, Gu Y, Taya C, Karasuyama H, Su MS, Rakic P, Flavell RA. 1998. Reduced apoptosis and cytochrome c-mediated caspase activation in mice lacking caspase 9. Cell 94:325–337.
Lavado A, Lagutin OV, Chow LM, Baker SJ, Oliver G. 2010. Prox1 is required for granule cell maturation and intermediate progenitor maintenance during brain neurogenesis. PLoS Biol 8:8.
LaVail JH, Cowan WM. 1971. The development of the chick optic tectum. I. Normal morphology and cytoarchitectonic development. Brain Res 28:391–419.
Logan M, Tabin C. 1998. Targeted gene misexpression in chick limb buds using avian replication-competent retroviruses. Methods 14:407–420.
Marin O, Rubenstein JL. 2001. A long, remarkable journey: tangential migration in the telencephalon. Nat Rev Neurosci 2:780–790.
Martini FJ, Valiente M, Lopez Bendito G, Szabo G, Moya F, Valdeolmillos M, Marin O. 2009. Biased selection of leading process branches mediates chemotaxis during tangential neuronal migration. Development 136:41–50.
McDonald PC, Fielding AB, Dedhar S. 2008. Integrin-linked kinase—essential roles in physiology and cancer biology. J Cell Sci 121(Pt 19):3121–3132.
Mollinari C, Ricci-Vitiani L, Pieri M, Lucantoni C, Rinaldi AM, Racaniello M, De Maria R, Zona C, Pallini R, Merlo D, Garaci E. 2009. Downregulation of thymosin beta4 in neural progenitor grafts promotes spinal cord regeneration. J Cell Sci 122(Pt 22):4195–4207.
Nieto MA, Patel K, Wilkinson DG. 1996. In situ hybridization analysis of chick embryos in whole mount and tissue sections. Methods Cell Biol 51:219–235.
Niewmierzycka A, Mills J, St-Arnaud R, Dedhar S, Reichardt LF. 2005. Integrin-linked kinase deletion from mouse cortex results in cortical lamination defects resembling cobblestone lissencephaly. J Neurosci 25:7022–7031.
Philp D, Nguyen M, Scheremeta B, St-Surin S, Villa AM, Orgel A, Kleinman HK, Elkin M. 2004. Thymosin beta4 increases hair growth by activation of hair follicle stem cells. Faseb J 18:385–387.
Rakic P. 1988. Defects of neuronal migration and the pathogenesis of cortical malformations. Prog Brain Res 73:15–37.
Rodriguez-Niedenfuhr M, Papoutsi M, Christ B, Nicolaides KH, von Kaisenberg CS, Tomarev SI, Wilting J. 2001. Prox1 is a marker of ectodermal placodes, endodermal compartments, lymphatic endothelium and lymphangioblasts. Anat Embryol (Berl) 204:399–406.
Roth LW, Bormann P, Bonnet A, Reinhard E. 1999. beta-Thymosin is required for axonal tract formation in developing zebrafish brain. Development 126:1365–1374.
Safer D, Elzinga M, Nachmias VT. 1991. Thymosin beta 4 and Fx, an actin-sequestering peptide, are indistinguishable. J Biol Chem 266:4029–4032.
Schlosshauer B, Dutting D, Wild M. 1990. Target-independent regulation of a novel growth associated protein in the visual system of the chicken. Development 109:395–409.
Schutte B, Reynders MM, Bosman FT, Blijham GH. 1987. Effect of tissue fixation on anti-bromodeoxyuridine immunohistochemistry. J Histochem Cytochem 35:1343–1345.
Smart N, Risebro CA, Melville AA, Moses K, Schwartz RJ, Chien KR, Riley PR. 2007. Thymosin beta4 induces adult

epicardial progenitor mobilization and neovascularization. Nature 445:177–182.

Snow RL, Robson JA. 1995. Migration and differentiation of neurons in the retina and optic tectum of the chick. Exp Neurol 134:13–24.

Wang WS, Chen PM, Hsiao HL, Ju SY, Su Y. 2003. Overexpression of the thymosin beta-4 gene is associated with malignant progression of SW480 colon cancer cells. Oncogene 22:3297–3306.

Wang WS, Chen PM, Hsiao HL, Wang HS, Liang WY, Su Y. 2004. Overexpression of the thymosin beta-4 gene is associated with increased invasion of SW480 colon carcinoma cells and the distant metastasis of human colorectal carcinoma. Oncogene 23:6666–6671.

Yang H, Cheng X, Yao Q, Li J, Ju G. 2008. The promotive effects of thymosin beta4 on neuronal survival and neurite outgrowth by upregulating L1 expression. Neurochem Res 33:2269–2280.

Yoshimatsu T, Kawaguchi D, Oishi K, Takeda K, Akira S, Masuyama N, Gotoh Y. 2006. Non-cell-autonomous action of STAT3 in maintenance of neural precursor cells in the mouse neocortex. Development 133:2553–2563.